Chemical Engineering Science 324 (2026) 123318

Contents lists available at ScienceDirect

Chemical Engineering Science

journal homepage: www.elsevier.com/locate/ces

Introducing a novel numerical model for describing the electrical potential in electrolyte solutions

D.E.A. van den Eertwegh [a], A. Pari [b], E.A.J.F. Peters [a], J.A.M. Kuipers [a], M.W. Baltussen [a,]

[a] Department of Chemical Engineering and Chemistry, Eindhoven University of Technology, Het Kranenveld 14, Eindhoven, 5612 AJ, the Netherlands
[b] Department of Process and Energy, Delft University of Technology, Leeghwaterstraat 39, Delft, 2628 CB, the Netherlands

ARTICLE INFO

Keywords:
Electrical potential
Nernst-Planck flux
Ion transport
Multivalent ions
Numerical simulation

ABSTRACT

The transport of ions is governed by a species conservation equation and the Nernst-Planck flux expression. The latter requires information on the electrical potential, for which an additional transport equation is required. Traditional numerical approaches, such as solving the Poisson equation or applying the electroneutrality condition, face limitations in their applicability. In this work, a new numerical model is introduced for the electrical potential that effectively functions as a numerical switch between the Poisson equation and the electroneutrality condition. This model is tested for three different scenarios: a small-scale system where charge separation is expected in a large part of the domain, a large-scale system where charge separation is significantly less important, and a multi-ion liquid junction system. This new numerical model is capable of producing accurate results for all the tested systems.

1. Introduction

The transport of ionic species is an important phenomenon that can be encountered in many different fields, ranging from biological systems to chemical applications. It is governed by a species conservation equation in combination with the Nernst-Planck flux expression. In addition to the species transport equations for the ions, an equation describing either the distribution of the electrical potential or the electrical field is required. To model these systems, several approaches can be found in the literature, each with their own assumptions and applications. Cohen and Cooley (1965) were among the first authors to numerically solve the system of equations for ion transport in a thin permeable membrane. They define a set of two equations: the Poisson equation and an equation for the total current density in the system, which are both defined in terms of the electrical field. Although these equations can be used to solve the separation of charge, Cohen and Cooley (1965) chose to use the electroneutrality assumption, which was first proposed by Planck (Jackson, 1974). This assumption entails that there can be no separation of charge. By employing this assumption, they reduce the Poisson equation to the electroneutrality condition. Even though this method no longer directly provides an expression for the electrical field, the equation for the total current density, which is used to close the system of equations, does contain the electrical field. However, these equations can also be solved without assuming electroneutrality, for example Scharfetter and Gummel (1969) solved the Poisson equation in terms of the electrical field directly and Brumleve and Buck (1978) only used the equation for the total current density. Subramaniam et al. (2019) determined via a comparison between the use of the electroneutrality condition and the Poisson equation in terms of the electrical potential for a lithium symmetric cell that both models produce viable results. It is mentioned that for the system under consideration, adoption of the electroneutrality condition is more efficient from a numerical point of view. Britz and Strutwolf (2014) simulated a liquid junction system using a variety of approaches: (i) using the Poisson equation in terms of the electrical potential, (ii) using the Poisson equation in terms of the electrical field, (iii) eliminating the Poisson equation by directly substituting it into the species conservation equations (and integrating it where required), and finally (iv) by assuming electroneutrality. As a fifth approach, Britz and Strutwolf (2014) considered eliminating one species transport equation using the Poisson equation. However, due to the complexity of the resulting derivatives, this approach was not pursued. It was found that methods (i)-(iii) are able to predict the development of the electrical potential over time, where methods (i) and (ii) were more accurate than method (iii). Method (iv), i.e. the electroneutrality condition, was not able to capture the development of the electrical potential. A summary of the presented methods is shown in Table 1.

E-mail address: m.w.baltussen@tue.nl (M.W. Baltussen).

https://doi.org/10.1016/j.ces.2026.123318
Received 26 September 2025; Received in revised form 14 December 2025; Accepted 5 January 2026
Available online 12 January 2026

Table 1
A summary of the methods presented in the introduction.

Approach	Advantage(s)	Disadvantage(s)	References
Total current density equation	Accurately predicts charge separation	Electrical current density should be known and numerically more difficult to solve	Cohen and Cooley (1965), Brumleve and Buck (1978)
Poisson equation	Accurately predicts charge separation	Numerically more difficult to solve	Cohen and Cooley (1965), Scharfetter and Gummel (1969), Britz and Strutwolf (2014), Subramaniam et al. (2019)
Substitution of Poisson equation	Can predict charge separation and eliminates one transport equation	Predicted charge separation is not accurate	Britz and Strutwolf (2014)
Electroneutrality assumption, electroneutrality condition	Numerically easier to solve	Cannot predict charge separation	Cohen and Cooley (1965), Britz and Strutwolf (2014), Subramaniam et al. (2019)

Nomenclature

Latin Letters

$\mathcal{F}$	Faraday constant
$\mathbf{i}$	(Total) current density
$\mathbf{i}_d$	Current density analogous the displacement current
$\mathbf{i}_q$	Current density caused by moving charges
$\mathbf{n}$	Molar flux
$\mathbf{u}$	Solvent velocity
c	Concentration
D	Diffusion coefficient
e	Elementary charge
L	Domain length
L_D	Debye length
N_t	Number of time steps
N_x	Number of grid cells
R	Universal gas constant
T	Temperature
t	Time
x	x-coordinate
z	Ionic charge

Greek Letters

Δ	Difference
ϕ	Electrical potential
$\tilde{\alpha}^2$	Ratio of length scales or time scales
ρ_c	(Charge) density
τ_d	Diffusive relaxation time
τ_e	Electric relaxation time
ϵ_0	Permittivity of free space
ϵ_r	Dielectric constant

Subscripts

0	Initial
i	Species
t	Time
x	x-direction

Superscripts

n	Current time step
$n+1$	Next time step

Abbreviations

CDS	Central differencing scheme
CF	Constant field
ENC	Electroneutrality condition
FVM	Finite Volume Method
LBM	Lattice Boltzmann Method
LBPM	Lattice Boltzmann Methods for Porous Media
PDE	Partial differential equation

As is evident from earlier reported studies, different systems require different approaches. The most flexible approach is to either use the Poisson equation or the equation for the total current density, as these equations are capable of predicting charge separation. However, depending on the specific system, these equations can prove to be difficult to solve from a numerical perspective, as the range of time and length scales to be captured is large due to the occurrence of charge separation. As an alternative, the electroneutrality condition can be used, which does not have this requirement. However, the electroneutrality condition is not capable of predicting the separation of charge and thus should be used with care.

In this work, a new numerical model for the treatment of the electrical potential is presented that applies to the transport of ionic species. The model effectively functions as a numerical switch between the Poisson equation and the electroneutrality condition. As such, this approach offers flexibility and can be used for several different systems, in contrast to the existing methods. In Section 2, an overview of the governing equations and the conventional methods for describing the electrical potential is given, followed by a description of the newly proposed numerical approach. In addition, an overview of the numerical treatment is given. Section 3 showcases the new numerical approach for different types of systems, comparing the results generated using the new model to the results generated using conventional models. Finally, the conclusions are presented in Section 4.

2. Methodology

In this section, the governing equations are introduced. This introduction includes a detailed description of the available models in literature for charged species transport and a description of the newly proposed model. In addition, an overview of the numerical treatment of the equations is given.

2.1. Governing equations

The concentration of an ion can be determined from a simple species conservation equation:

$$\frac{\partial c_i}{\partial t} + \nabla \cdot \mathbf{n}_i = 0. \tag{1}$$

Here, c is the concentration, t the time and $\mathbf{n}$ the molar flux. The subscript i refers to a specific species. The total molar flux is given by a combination of the Nernst-Planck flux and a convective flux:

$$\mathbf{n}_i = -D_i \nabla c_i - z_i \frac{D_i}{RT} \mathcal{F} c_i \nabla \phi + \mathbf{u} c_i. \tag{2}$$

In this equation, D is the diffusion coefficient, z the signed ionic charge in units of e, $\mathcal{F}$ the Faraday constant, R the universal gas constant, T the temperature, ϕ the electrical potential and $\mathbf{u}$ the velocity of the solvent. The right-hand side of Eq. (2) consists of three separate contributions:

(Fickian) diffusion, electromigration and convective transport, respectively.

Apart from the species equations, a transport equation for the electrical potential is required to close the system of equations. To this end, the Poisson equation can be used:

$$-\nabla \cdot \left(\varepsilon_0 \varepsilon_r \nabla \phi\right) = \rho_c, \tag{3}$$

where ε_0 is the permittivity of free space, ε_r the dielectric constant of the solvent and ρ_c the charge density. The Poisson equation originates from the field of electrostatics. The usage of electrostatics rather than electrodynamics can be justified, considering that the timescale for the formation of an electrical field is significantly smaller than the timescale for species transport. For an electrolyte solution, the charge density ρ_c is given by:

$$\rho_c = \mathcal{F} \sum_i^N z_i c_i, \tag{4}$$

where N is the total number of species.

Different approximations can be derived from the Poisson equation. To this end, it is useful to consider the Poisson equation in its dimensionless form, using the following dimensionless operator and quantities:

$$\tilde{\nabla} = \frac{1}{L}\nabla, \tag{5a}$$

$$\tilde{c} = \frac{1}{c_0} c, \tag{5b}$$

$$\tilde{\phi} = \frac{\mathcal{F}}{RT}\phi. \tag{5c}$$

Note that the dimensionless quantities are indicated by a tilde. Using these expressions in combination with Eq. (3) with a constant $\varepsilon_0\varepsilon_r$ yields

$$\tilde{\alpha}^2 \tilde{\nabla}^2 \tilde{\phi} = \sum_i^N z_i \tilde{c}_i, \text{ where } \tilde{\alpha}^2 = \frac{\varepsilon_0 \varepsilon_r RT}{\mathcal{F}^2 L^2 c_0}. \tag{6}$$

The parameter $\tilde{\alpha}^2$ can be interpreted both as the ratio of the Debye length, L_D, to the system size and as the ratio of an electric relaxation time, τ_e, to a diffusive relaxation time, τ_d, (Mafé et al., 1986):

$$\tilde{\alpha}^2 = \left(\frac{L_D}{L}\right)^2 = \frac{L_D^2/D}{L^2/D} = \frac{\tau_e}{\tau_d}, \tag{7a}$$

$$L_D = \sqrt{\frac{\varepsilon_0 \varepsilon_r RT}{\mathcal{F}^2 c_0}}, \tag{7b}$$

$$\tau_e = \frac{L_D^2}{D}, \tag{7c}$$

$$\tau_d = \frac{L^2}{D}. \tag{7d}$$

When $\tilde{\alpha}^2$ is small, the following (dimensional) approximation is obtained from Eq. (6):

$$\sum_i^N z_i c_i = 0. \tag{8}$$

This is known as the electroneutrality condition (ENC). According to ENC, charge separation cannot take place within the domain. The small value of $\tilde{\alpha}^2$ implies that ENC is only a good approximation if the system size is significantly larger than the Debye length $L \gg L_D$ (or similarly, the electric relaxation time is significantly smaller than the diffusive relaxation time $\tau_e \ll \tau_d$). This is in accordance with the work of MacGillivray (1968)[1], in which it is shown that ENC is the zeroth order approximation of the perturbation expansion around $\tilde{\alpha}^2$.

When considering the limit of $\tilde{\alpha}^2$ approaching infinity, Goldman's constant field (CF) approximation (Goldman, 1943) is obtained from Eq. (6):

$$\nabla^2 \phi = 0. \tag{9}$$

This equation effectively states that the electrical field is constant. MacGillivray and Hare (1969) showed that the CF approximation is the zeroth order approximation of the perturbation expansion about $1/\tilde{\alpha}^2$, supporting the previously mentioned limit. However, Kato (1995) showed that the CF approximation can be used for higher values of $1/\tilde{\alpha}^2$, with $1/\tilde{\alpha}^2 = 1.7$ giving an error of approximately 10%.

An alternative to the Poisson equation is the equation for the electrical current density, which was used first by Cohen and Cooley (1965):

$$\mathbf{i} = \mathbf{i}_q + \mathbf{i}_d, \tag{10}$$

where

$$\mathbf{i}_q = \mathcal{F} \sum_i^N z_i \mathbf{n}_i, \tag{11a}$$

$$\mathbf{i}_d = -\varepsilon_0 \varepsilon_r \frac{\partial \nabla \phi}{\partial t}. \tag{11b}$$

Here, $\mathbf{i}$ is the resulting current density, $\mathbf{i}_q$ the current density arising from the movement of ions due to gradients in concentration and electrical potential and $\mathbf{i}_d$ is the displacement current density[2] The derivation of Eq. (10) is shown by both Buck (1984) and Mafé et al. (1988), each using different physical principles.

To further analyse the equation for the electrical current density, it is useful to consider its dimensionless form using the following three dimensionless quantities in Eqs. 12a–12c in addition to those given in Eqs. 5a–5c:

$$\tilde{\mathbf{i}} = \frac{L}{Dc_0\mathcal{F}}\mathbf{i}, \tag{12a}$$

$$\tilde{\mathbf{n}}_i = \frac{L}{Dc_0}\mathbf{n}_i, \tag{12b}$$

$$\tilde{t} = \frac{D}{L^2} t. \tag{12c}$$

$$\tilde{\mathbf{i}} = \sum_i^N z_i \tilde{\mathbf{n}}_i - \tilde{\alpha}^2 \frac{\partial \tilde{\nabla} \tilde{\phi}}{\partial \tilde{t}}. \tag{13}$$

Analogous to the previous analysis, $\mathbf{i}_d$ can be neglected when $\tilde{\alpha}^2$ approaches zero, yielding $\mathbf{i} = \mathbf{i}_q$. Substituting the Nernst-Planck flux (Eq. (2)) into this equation, using ENC (Eq. (8)) and rewriting for the gradient of the electrical potential yields:

$$\nabla \phi = \frac{\frac{\mathbf{i}}{\mathcal{F}} + \sum_i^N z_i D_i \nabla c_i}{-\frac{\mathcal{F}}{RT}\sum_i^N z_i^2 D_i c_i}. \tag{14}$$

This equation for the electrical potential is valid in case ENC holds. Similarly, CF approximation (Eq. (9)) is obtained when $\tilde{\alpha}^2$ approaches infinity.

Each of the equations (or closures) for the electrical potential defined above has its advantages and disadvantages. The Poisson equation generally provides the highest flexibility, as it can produce viable results in every situation. However, the numerical treatment of the equation requires a relatively small time step size and grid size, which might be undesirable depending on the considered problem. ENC is only valid under specific conditions, but significantly simplifies the numerical treatment. As ENC does not determine the electrical potential by itself, Eq. (14) should be used to calculate the potential field. The advantages and disadvantages for CF approximation are similar to ENC, except that the

[1] In the work of MacGillivray (1968), $\tilde{\alpha}^2$ is defined as $\left(\varepsilon_0\varepsilon_r RT/\left(\mathcal{F}^2 L^2 c_0\right)\right)\left(\Delta c/c_0\right)$. However, this does not change the result obtained from the perturbation analysis.

[2] Unlike $\mathbf{i}_q$, the displacement current density $\mathbf{i}_d$ does not represent the physical transport of charge carriers. Instead, it describes the effect from the time-varying electrical field and is used to capture the capacitive behaviour of the electrochemical double layer.

electrical potential is directly calculated. Finally, the model using the electrical current density, Eqs. 10–13, is also capable of producing viable results in every situation. However, it requires the value for the electrical current density, which is not always readily available. To overcome some of these disadvantages, a new numerical approach is presented in this work. This approach is based on the continuity equation for electrical charge, which is given by:

$$\frac{\partial \rho_c}{\partial t} + \nabla \cdot \mathbf{i}_q = 0. \tag{15}$$

Since this equation is derived by multiplying each species conservation equation (Eq. (1)) by $z_i\mathcal{F}$ and summing them, it is not unique and cannot be used in its current form. To address this, the Poisson equation (Eq. (3)) is numerically embedded into Eq. (15), as further discussed in Section 2.2. The method will effectively behave as a numerical switch between the Poisson equation and the transport equation for the electrical potential that is valid in case ENC holds.

2.2. Numerical treatment

For the discretisation of the partial differential equations (PDEs), a cell-centred Finite Volume Method (FVM) is used. All simulations are performed using the in-house software FoxBerry.

For each of the ionic species, the species continuity equation (Eq. (1)) is solved in combination with the Nernst-Planck flux (Eq. (2)). The time derivative is treated using a first-order accurate implicit Euler scheme, while both the (Fickian) diffusion flux and the electromigrative flux are discretised in space using a second-order accurate central differencing scheme (CDS). The non-linear electromigrative flux term is included by treating the concentration explicitly and the potential implicitly.

For the electrical potential, the Poisson equation (Eq. (3)), the equation obtained from ENC (Eq. (14)) or the new approach based on the continuity equation for the electrical charge (Eq. (15)) can be used. CF (Eq. (9)) is not considered, as this approximation is not valid for the systems under consideration.

In the discretisation of the Poisson equation CDS is used for the second-order spatial derivative. All terms in the equation are treated implicitly.

In case of ENC, the following equation is obtained by combining equations Eqs. (1), (2) and (8):

$$-\nabla \cdot \left(\frac{\mathcal{F}}{RT} \left(\sum_i^N z_i^2 D_i c_i \right) \nabla \phi \right) = \nabla \cdot \left(\sum_i^N z_i D_i \nabla c_i \right). \tag{16}$$

This equation will hereafter be referred to as the electroneutrality equation. For this equation, the second-order spatial derivatives are treated using CDS. The non-linear dependency on the left-hand side is included by treating the concentrations explicitly and the potential implicitly. The right-hand side is treated fully implicitly.

For the approach based on the continuity equation for electrical charge, the Poisson equation is numerically embedded into Eq. (15). To this end, Eq. (3) is derived to the time to obtain:

$$\frac{\partial \rho_c}{\partial t} = -\frac{\partial}{\partial t} \left(\nabla \cdot \left(\varepsilon_0 \varepsilon_r \nabla \phi \right) \right). \tag{17}$$

The derivative of the potential to the time on the right-hand side of Eq. (17) is discretised using a first-order accurate approximation:

$$\frac{\partial \rho_c}{\partial t} = -\frac{\nabla \cdot \left(\varepsilon_0 \varepsilon_r \nabla \phi^{n+1} \right) - \nabla \cdot \left(\varepsilon_0 \varepsilon_r \nabla \phi^{n} \right)}{\Delta t}. \tag{18}$$

Here, the superscript n refers to the current time step and the superscript $n+1$ to the next time step. Evaluating the Poisson equation, including the definition for the charge density given in Eq. (4), at time step n yields the following relation:

$$-\nabla \cdot \left(\varepsilon_0 \varepsilon_r \nabla \phi^{n} \right) = \mathcal{F} \sum_i^N z_i c_i^n. \tag{19}$$

This relation can be substituted into Eq. (18) to obtain the following expression for the derivative of the charge density to time:

$$\frac{\partial \rho_c}{\partial t} = \frac{-\nabla \cdot \left(\varepsilon_0 \varepsilon_r \nabla \phi^{n+1} \right) - \mathcal{F} \sum_i^N z_i c_i^n}{\Delta t}. \tag{20}$$

Using Eqs. (2), (11a) and (20), Eq. (15) can be rewritten to:

$$\begin{aligned} \frac{-\nabla \cdot \left(\varepsilon_0 \varepsilon_r \nabla \phi^{n+1} \right) - \mathcal{F} \sum_i^N z_i c_i^n}{\Delta t} = \mathcal{F} \Bigg[& \nabla \cdot \left(\sum_i^N z_i D_i \nabla c_i \right) \\ & + \nabla \cdot \left(\frac{\mathcal{F}}{RT} \left(\sum_i^N z_i^2 D_i c_i \right) \nabla \phi^{n+1} \right) \\ & - \nabla \cdot \left(\mathbf{u} \sum_i^N z_i c_i \right) \Bigg]. \end{aligned} \tag{21}$$

This equation will be referred to as the charge conservation equation. For the charge conservation equation, the time step size effectively works as a numerical switch and can be viewed as an asymptotic preserving scheme (Larsen et al., 1987; Larsen and Morel, 1989; Jin and Levermore, 1996; Jin, 1999; Degond et al., 2010; Hu et al., 2017; Anguill et al., 2022): the Poisson equation is dominant for small time step sizes, while for larger time step sizes the behaviour is governed by the electroneutrality equation. Note that the derivation presented here generalises to higher-order approximations for the time discretisation. For the second-order spatial derivatives in Eq. (21), CDS is used. The first term on the right-hand side is treated fully implicitly, while the non-linearity in the second term is overcome by treating the concentrations explicitly and the electrical potential implicitly. The last term on the right-hand side is not taken into account, as it is assumed that $\mathbf{u} = 0$ for all systems presented in this work.

The combination of the species equations and an equation for the electrical potential is solved in a coupled fashion using the BiCGStab2 iterative solver (Masterov, 2019) in combination with an incomplete LU preconditioner from Trilinos (Prokopenko et al., 2016; Team, 2020) (the maximum number of iterations was set to 10^4 and the convergence criterion used is 10^{-14})[3]. The boundary conditions are described using a first-order fully coupled description. When the electromigrative flux expression is used as (part of) a boundary condition, the concentration is treated explicitly, while the electrical potential is treated implicitly. The values used in the boundary conditions are updated every time step when required.

It is noted that mathematical simplifications exist when ENC holds and a binary electrolyte is used, without introducing additional assumptions (Newman and Thomas-Alyea, 2004; Fuller and Harb, 2018). In this case, it is possible to fully eliminate the electrical potential from the species transport equation, yielding a single transient convection-diffusion equation that is valid for both ionic species. In addition, ENC (Eq. (8)) allows for the elimination of one species transport equation in systems with three or more ionic species. The concentration of the eliminated species can then be determined as a function of the others. In this work, it is chosen to follow neither of the aforementioned mathematical simplifications in order to have an objective comparison between the different transport equations for the electrical potential.

3. Results

To demonstrate the versatility of the newly proposed numerical model, three test cases are considered: a small-scale system where charge separation is expected in most of the domain, a large-scale system where charge separation is significantly less important, and a multi-ion liquid junction system. For the latter system, the importance of charge separation is varied by changing the system parameters, and the effect

[3] Note that no under-relaxation was used in the numerical solving procedure.

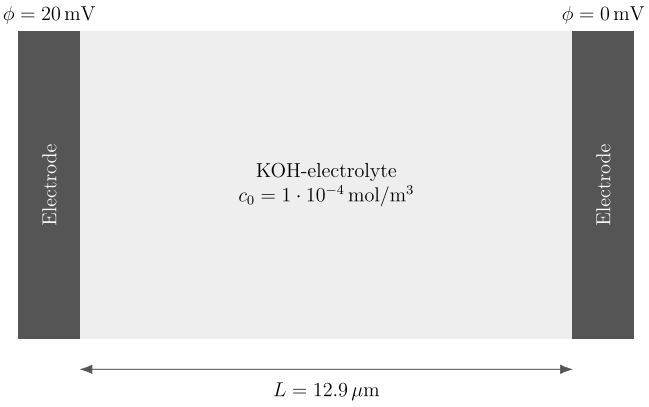

Fig. 1. A schematic overview of the small-scale system.

Table 2
Simulation parameters for the small-scale system.

Description		Value	
Ionic species	i	$\{K^+, OH^-\}$	
Ionic charge	z_i	$\{+1, -1\}$	
Diffusion coefficient	D_i	$\{1.96 \cdot 10^{-9}, 5.27 \cdot 10^{-9}\}$	m^2/s
Initial KOH concentration	c_0	$\{10^{-4}, 10^{-4}\}$	mol/m^3
Dielectric constant solvent	ϵ_r	80.2	
Temperature	T	293.15	K
Applied potential difference	$\Delta\phi$	$2 \cdot 10^{-2}$	V
Domain length	L	$12.9 \cdot 10^{-6}$	m
Number of grid cells	N_x	110	
Time step size	Δt	$1.3 \cdot 10^{-6}$	s
Number of time steps	N_t	28800	

of the electrical potential equation on the predicted liquid junction potential is evaluated. It is noted that all simulations were performed in 2D, while the effect is only studied in a single coordinate direction. A zero-gradient boundary condition is applied for both the ionic species and the electrical potential in the other coordinate direction, such that no profiles will be observed. Two grid cells were used for this coordinate direction.

3.1. Small-scale system

The small-scale system consists of a potassium hydroxide electrolyte surrounded by two inert electrodes, which is shown schematically in Fig. 1. The parameters used in this simulation are given in Table 2. Based on a time and grid dependency study, both the chosen time step size and grid size show a negligible error of $\mathcal{O}(10^{-3}\%)$.

The simulations are performed using the Poisson equation and the newly developed charge conservation equation for the electrical potential. The electroneutrality equation is not used for this case, as this method will not be able to predict the charge separation based on its definition.

To verify the implementation, the simulation results will be compared against those obtained from the ion transport model in the Lattice Boltzmann Methods for Porous Media (LBPM) code (Tang et al., 2023). LBPM is a highly parallelised GPU-enabled open-source software package which employs the lattice Boltzmann method (LBM) to model mesoscale phenomena, including ion transport at a scale where charge separation is significant and must be resolved. This is achieved by coupling the Nernst-Planck flux (Eq. (2)) and the Poisson equation (Eq. (3)). Since LBM is inherently suitable for parabolic PDEs, whereas the Poisson equation is elliptical in nature, an ad hoc temporal term is added to the original Poisson equation:

$$\frac{\partial \phi}{\partial t} = \nabla^2 \phi + \frac{\rho_c}{\epsilon_0 \epsilon_r}. \tag{22}$$

Table 3
Simulation parameters for the large-scale system.

Description		Value	
Ionic species	i	$\{Li^+, PF_6^-\}$	
Ionic charge	z_i	$\{+1, -1\}$	
Diffusion coefficient	D_i	$\{4.0 \cdot 10^{-10}, 4.0 \cdot 10^{-9}\}$	m^2/s
Initial $LiPF_6$ concentration	c_0	{500, 500}	mol/m^3
Dielectric constant solvent	ϵ_r	16.8	
Temperature	T	298.15	K
Domain length	L	$7.5 \cdot 10^{-4}$	m
Number of grid cells	N_x	320	
Time step size	Δt	$1.0 \cdot 10^{-2}$	s
Number of time steps	N_t	45000	

This modified Poisson equation is solved until a pseudo steady-state within a time step, similar to how it is done in the work of Tang et al. (2023). It is noted that while the dimension of the temporal term does not match the dimensions of the two remaining terms, the value of this term will be equal to zero at the pseudo steady-state and thus no problem is introduced. The electrical potential obtained from Eq. (22) is used to solve for the Nernst-Planck flux, which yields the ionic concentration profiles.

The simulation results generated using the charge conservation equation are shown in Fig. 2. The data generated using the Poisson equation shows very similar results. To quantify the difference between these two models, the L_∞ norm is calculated as:

$$L_\infty = \max\left(\left|\frac{c_{i,\text{charge conservation}} - c_{i,\text{Poisson}}}{c_{i,\text{charge conservation}}}\right|\right). \tag{23}$$

The L_∞ norm is calculated for both ions, and the maximum value is found to be $3.5 \cdot 10^{-4}\%$. This difference is found at the final time step.

As expected, the positively charged potassium ion is repelled by the electrode with the highest electrical potential, while it is attracted by the electrode with the lowest electrical potential. The opposite is true for the hydroxide ion, as this ion is negatively charged. As a result of the rearrangement of the ions, the electrical potential profile changes. Initially, a linear profile is observed between the two electrodes, which develops to a flat profile in the middle of the domain with significant gradients near both electrodes. This suggests a strong electrical field near the electrodes and a vanishing field at the centre of the domain, which is a characteristic feature of electrode shielding.

Comparing the simulation results with those from LBPM reveals a similar (transient) trend. However, in contrast to LBPM, the FVM results show slightly smaller slopes near the electrodes for both ion concentration profiles and the electrical potential profile, suggesting that FVM predicts a lower degree of shielding. While it is unclear which method provides more accurate results (as there is no independent judge), the difference between them is minor, supporting the conclusion that the implementation is correct.

3.2. Large-scale system

For the large-scale system, the lithium symmetric cell system described by Subramaniam et al. (2019) is used, which is schematically shown in Fig. 3.

The simulation parameters can be found in Table 3. The boundary conditions are taken from Subramaniam et al. (2019).

After performing the time and grid dependency studies, the chosen time step size and grid size both show a negligible error of $\mathcal{O}(10^{-4}\%)$.

For this test case, the simulations are performed using the electroneutrality equation and the charge conservation equation. The Poisson equation is not reported, as divergence was observed for the reported grid size and time step size. The simulation results for the charge conservation equation can be found in Fig. 4. Visually indistinguishable results are obtained when using the electroneutrality equation. To quantify the performance of both models, the generated data is compared to

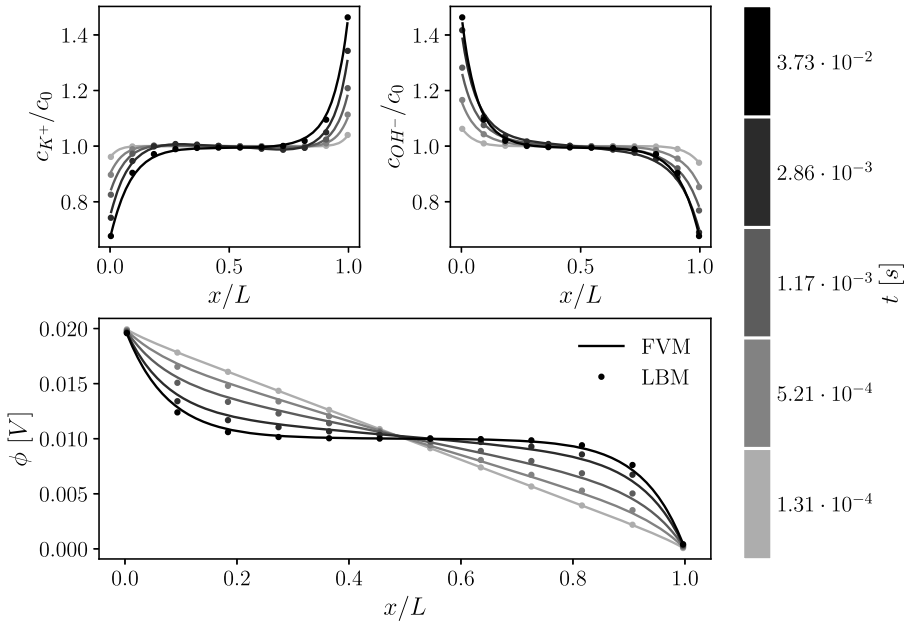

Fig. 2. The simulation results for the small-scale system, obtained using the charge conservation equation for the electrical potential. The results are compared to the results obtained using LBPM.

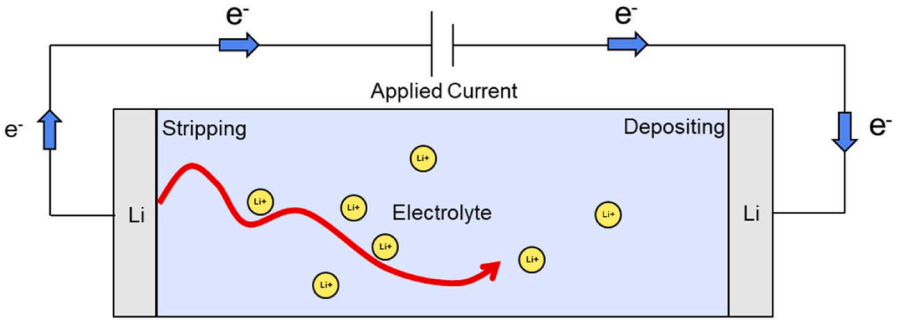

Fig. 3. A schematic overview of the large-scale system (Subramaniam et al., 2019).

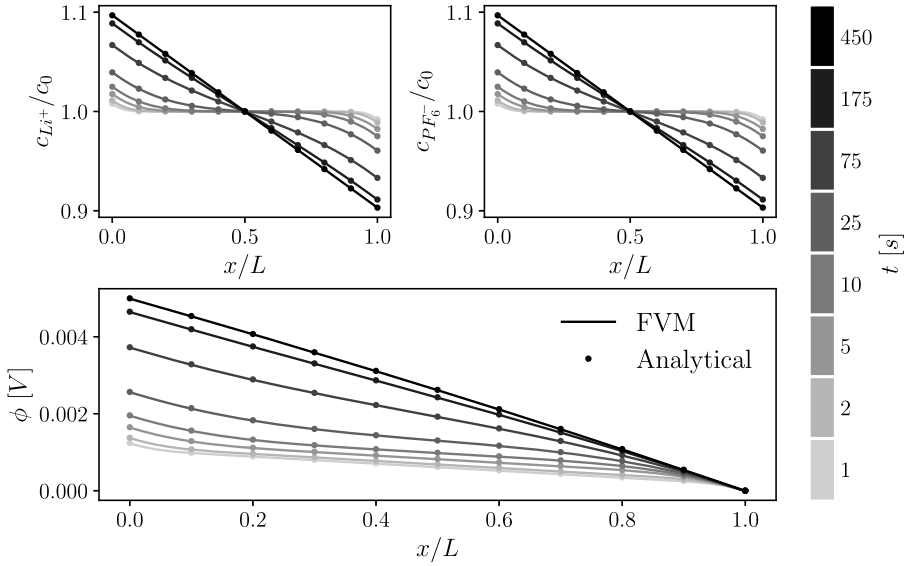

Fig. 4. The simulation results for the large-scale system, obtained using the charge conservation equation for the electrical potential.

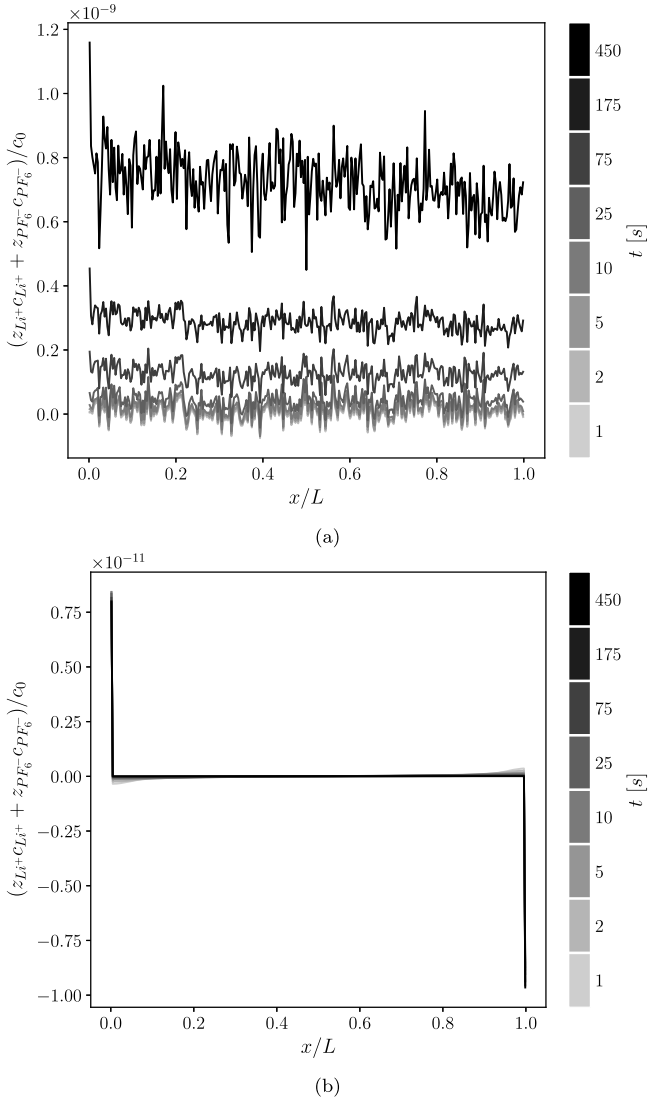

Fig. 5. The dimensionless ENC retrieved from the simulations when using (a) the electrical potential in case of the ENC and (b) the charge conservation equation.

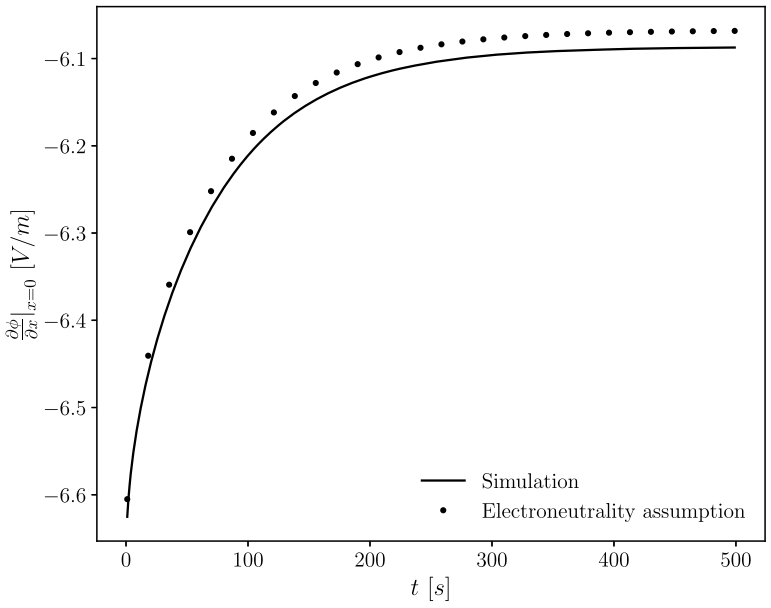

Fig. 6. The electrical potential gradient at the left side of the domain, obtained using the charge conservation equation.

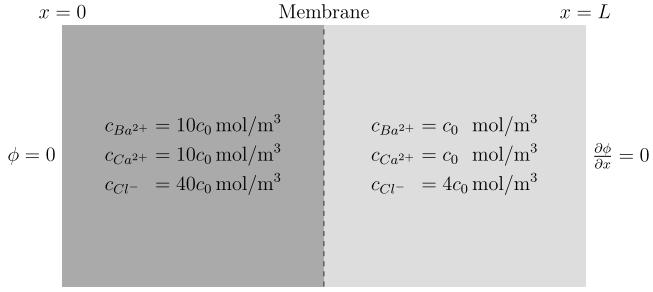

Fig. 7. A schematic overview of the liquid junction system.

the analytical solution for the ion concentrations reported by Subramaniam et al. (2019), which is based on ENC for a binary salt. The L_∞ norm is calculated for each ion as:

$$L_\infty = \max\left(\left|\frac{c_{i,\text{model}} - c_{i,\text{analytical}}}{c_{i,\text{analytical}}}\right|\right). \tag{24}$$

Considering all time steps, a maximum of $1.7 \cdot 10^{-5}$% was obtained for both models. This indicates a slightly better performance compared to the time and grid dependency studies.

Due to the stripping of lithium ions on the left side of the system, an increase in the lithium ion concentration is observed. The increase of the ion concentration is time-dependent, and reaches a maximum of approximately 110% of the initial lithium ion concentration. The opposite is true for the right side of the domain, where a decrease in lithium ions is observed. The concentration profile of the hexafluorophosphate counter-ion closely follows the concentration profile of the lithium ion, hinting at electroneutrality. For both ionic species, the simulation results nicely match the analytical results. The electrical potential slowly develops in a non-linear fashion as a result of the imposed current. In steady state, it shows a linear profile with a potential difference of 5 mV over the electrolyte solution. The analytical values for the electrical potential profile are obtained by numerically integrating Eq. (14), taking into account the analytical formula for the ion concentrations as found in the work of Subramaniam et al. (2019). As can be seen, a good agreement is found.

Both models predict an insignificant residual charge (see Fig. 5), implying that electroneutrality holds. For the electroneutrality equation, the observed profile is approximately flat and increases marginally with time, which can be explained by an accumulation of errors. For the charge conservation equation, an accumulation of residual charge can be found at both of the boundaries of the system, which could be explained by the numerical inclusion of the Poisson equation. The centre of the domain shows a negligible residual charge, as expected. In general, the charge conservation equation seems to drive the system towards electroneutrality.

Following Subramaniam et al. (2019), a zero-gradient boundary condition for the electrical potential is applied at the left side of the domain ($x = 0$). However, as is apparent from Fig. 4, a non-zero gradient of the electrical potential is observed in that region. To confirm whether the resulting electrical potential profile shows the expected behaviour, the numerical gradient is compared to the analytical gradient assuming electroneutrality (see Eq. (14)). A three point stencil is used to determine the numerical gradient at the boundary, taking into account that the first internal cell node is located half of the grid spacing inside the domain:

$$\frac{d\phi}{dx}\Big|_{x=0} = \frac{-2\phi_1 + 3\phi_2 - \phi_3}{\Delta x}, \tag{25}$$

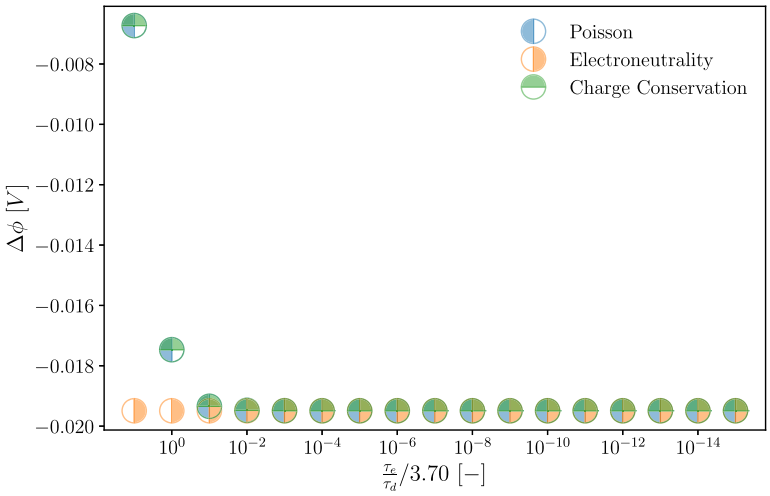

Fig. 8. The simulation results for the liquid junction system.

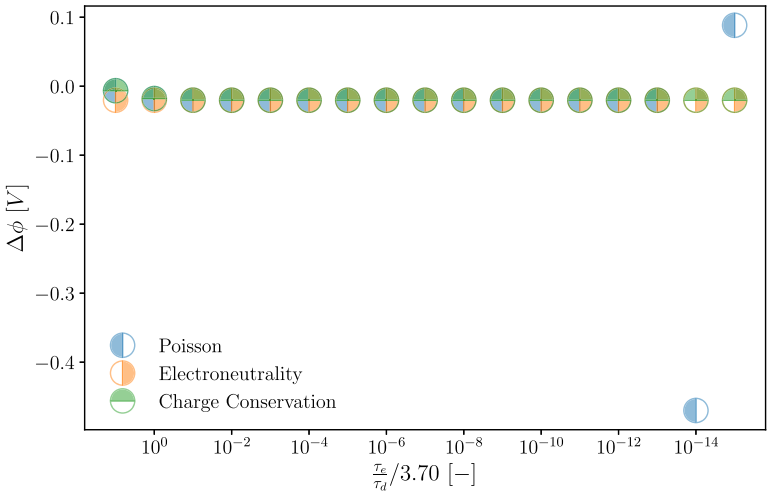

Fig. 9. The simulation results for the liquid junction system for a larger time step size of $\Delta t = 5 \cdot 10^{-3}$ s. As can be observed, the Poisson equation is not capable of producing valid results for small values of $\tilde{\alpha}^2$.

where ϕ_1, ϕ_2 and ϕ_3 are the potential values at the first, second and third internal cell nodes, respectively, and Δx is the uniform grid spacing. The result for the charge conservation equation can be found in Fig. 6. The results generated using the electroneutrality equation are visually identical and therefore not shown.

As can be observed, the numerical potential gradient follows the analytical gradient. The error is estimated using the L_∞ norm:

$$L_\infty = \max\left(\left|\frac{\frac{d\phi}{dx}\Big|_{x=0,\text{model}} - \frac{d\phi}{dx}\Big|_{x=0,\text{analytical}}}{\frac{d\phi}{dx}\Big|_{x=0,\text{analytical}}}\right|\right), \tag{26}$$

showing a maximum value of 0.3%.

3.3. Liquid junction system

The last system is a liquid junction system based on the work of Mafé et al. (1986). The system consists of two barium chloride-calcium chloride electrolyte solutions of different concentrations, separated by a membrane, as schematically shown in Fig. 7. At the start of the simulation, the membrane is removed and the solutions are allowed to mix. A potential difference is formed due to a competition between the diffusion fluxes, separating the ionic species, and the electromigration fluxes, keeping the ionic species close together. This liquid junction potential reaches a pseudo steady-state, which is disrupted when the boundary conditions start to influence the ions. The value of the liquid junction potential depends on the parameters used in the system and can be expressed using the ratio of the electric relaxation time to the diffusive relaxation time, Eqs. (7c) and (7d) respectively. To tune this ratio, the concentration c_0 (see Fig. 7) is varied between $5 \cdot 10^{-8}$ to $5 \cdot 10^{8}$ mol/m^3. While the upper limit far exceeds the physical solubility of the salts, the results are purely used for demonstrative purposes.

The parameters used in the simulations can be found in Table 4.

Table 4
Simulation parameters for the liquid junction system.

Description		Value	
Ionic species	i	{Ba^{2+}, Ca^{2+}, Cl^-}	
Ionic charge	z_i	{+2, +2, −1}	
Diffusion coefficient	D_i	$\{8.48 \cdot 10^{-10}, 7.93 \cdot 10^{-10}, 2.03 \cdot 10^{-9}\}$	m^2/s
Initial salt concentration	c_0	$\{5 \cdot 10^{-8}, \ldots, 5 \cdot 10^{8}\}$	mol/m^3
Dielectric constant solvent	ϵ_r	78.4	
Temperature	T	298.15	K
Domain length	L	$1 \cdot 10^{-4}$	m
Number of grid cells	N_x	100	
Time step size	Δt	$1 \cdot 10^{-4}$	s
Number of time steps	N_t	300	

As previously mentioned, the boundary conditions for the species should not affect the pseudo steady-state results and can thus be arbitrarily chosen. In this work, no-flux boundary conditions are used on both sides of the domain. For the potential, it is important to fix the value using a Dirichlet boundary condition on one side of the domain and to allow for development of the potential with a Neumann boundary condition equal to zero on the other side. The time and grid dependency studies were performed both for the highest and lowest values for the concentration c_0. The values reported in Table 4 show an error of $\mathcal{O}(10^{-1})$% for both the time step size and grid size.

The simulation results of all three models for the electrical potential are shown in Fig. 8. For small values of $\tilde{\alpha}^2$, all models predict similar results. However, the results obtained for high values of $\tilde{\alpha}^2$ using the electroneutrality equation are different from the results computed using the Poisson equation and the charge conservation equation. This result is expected, as electroneutrality holds only when $\tilde{\alpha}^2$ is small. Using the electroneutrality equation, the liquid junction potential is independent of $\tilde{\alpha}^2$, reflecting the strict enforcement of charge neutrality.

Results obtained by solving the Poisson equation and the charge conservation equation are very similar. The advantage of using the charge conservation over the Poisson equation is apparent when numerically resolving the process of charge separation becomes increasingly more difficult, for example by increasing the time step size to $\Delta t = 5 \cdot 10^{-3}$ s which is shown in Fig. 9.[4] In this case, the Poisson equation does not yield viable results for low values of $\tilde{\alpha}^2$, while the charge conservation equation and the electroneutrality equation are able to produce accurate results. This can be explained by the effective switching in the charge conservation equation to the electroneutrality equation.

4. Conclusion

A new numerical model for the treatment of the electrical potential, referred to as the charge conservation equation, was presented in this work. This model effectively functions as a numerical switch between the Poisson equation and the electroneutrality equation. The charge conservation equation has been tested for three different systems: a small-scale system where charge separation is expected in most of the domain, a large-scale system where charge separation is significantly less important, and a multi-ion liquid junction system where the importance of charge separation depends on the chosen parameters. The results generated using the charge conservation equation were compared to the results generated by the Poisson equation and/or the electroneutrality equation, depending on the system. It was found that usage of the charge conservation equation produces accurate results for each of the systems, while usage of both the Poisson equation and the electroneutrality equation fails to produce accurate results in all cases. In comparison to the Poisson equation, the charge conservation equation is more convenient from a numerical viewpoint as it circumvents to resolve the time and length scales of charge separation. Compared to the electroneutrality equation, the charge conservation equation does not inherently assume electroneutrality.

CRediT authorship contribution statement

D.E.A. van den Eertwegh: Writing – original draft, Visualization, Validation, Software, Methodology, Investigation, Formal analysis, Conceptualization; **A. Pari:** Writing – review & editing, Visualization, Methodology, Formal analysis, Data curation; **E.A.J.F. Peters:** Writing – review & editing, Methodology, Investigation, Formal analysis; **J.A.M. Kuipers:** Writing – review & editing, Supervision, Resources, Methodology, Funding acquisition, Conceptualization; **M.W. Baltussen:** Writing – review & editing, Visualization, Supervision, Software, Project administration, Methodology, Funding acquisition, Formal analysis, Conceptualization.

Data availability

Data will be made available on request.

Declaration of competing interest

The authors declare the following financial interests/personal relationships which may be considered as potential competing interests: D.E.A. van den Eertwegh, A. Pari, J.A.M. Kuipers and M.W. Baltussen reports financial support was provided by Dutch Research Council. D.E.A. van den Eertwegh, A. Pari, J.A.M. Kuipers and M.W. Baltussen reports financial support was provided by Shell. D.E.A. van den Eertwegh, A. Pari, J.A.M. Kuipers and M.W. Baltussen reports financial support was provided by Nobian Holding BV. D.E.A. van den Eertwegh, A. Pari, J.A.M. Kuipers and M.W. Baltussen reports financial support was provided by Nouryon Chemicals BV. If there are other authors, they declare that they have no known competing financial interests or personal relationships that could have appeared to influence the work reported in this paper.

Acknowlegdement

This publication is part of the project Bubble Dynamics in Electrolysis (with project number 741.019.201) of the research programme Meerfase-stroming voor verduurzaming van de industrie which is (partly) financed by the Dutch Research Council (NWO). This research has industrial funding by Shell, Nobian and Nouryon.

References

Anguill, P., Cargo, P., Énaux, C., Hoch, P., Labourasse, E., Samba, G., 2022. An asymptotic preserving method for the linear transport equation on general meshes. J. Comput. Phys. 450, 110859.
Britz, D., Strutwolf, J., 2014. Several ways to simulate time dependent liquid junction potentials by finite differences. Electrochim. Acta 137, 328–335.
Brumleve, T.R., Buck, R.P., 1978. Numerical solution of the Nernst-Planck and poisson equation system with applications to membrane electrochemistry and solid state physics. J. Electroanal. Chem. Interfacial Electrochem. 90 (1), 1–31.
Buck, R.P., 1984. Kinetics of bulk and interfacial ionic motion: microscopic bases and limits for the Nernst-Planck equation applied to membrane systems. J. Memb. Sci. 17 (1), 1–62.
Cohen, H., Cooley, J.W., 1965. The numerical solution of the time-dependent Nernst-Planck equations. Biophys. J. 5 (2), 145–162.
Degond, P., Deluzet, F., Navoret, L., Sun, A.-B., Vignal, M.-H., 2010. Asymptotic-preserving particle-in-cell method for the vlasov-poisson system near quasineutrality. J. Comput. Phys. 229 (16), 5630–5652.
Fuller, T.F., Harb, J.N., 2018. Electrochemical Engineering. John Wiley & Sons. 1 edition.
Goldman, D.E., 1943. Potential, impedance, and rectification in membranes. J. Gen. Physiol. 27 (1), 37–60.
Hu, J., Jin, S., Li, Q., 2017. Chapter 5 - asymptotic-preserving schemes for multiscale hyperbolic and kinetic equations. In: Abgrall, R., Shu, C.-W. (Eds.), Handbook of Numerical Methods for Hyperbolic Problems. Elsevier. Vol. 18 of *Handbook of Numerical Analysis*, pp. 103–129.
Jackson, J.L., 1974. Charge neutrality in electrolytic solutions and the liquid junction potential. J. Phys. Chem. 78 (20), 2060–2064.
Jin, S., 1999. Efficient asymptotic-preserving (AP) schemes for some multiscale kinetic equations. SIAM J. Scient. Comput. 21 (2), 441–454.
Jin, S., Levermore, C.D., 1996. Numerical schemes for hyperbolic conservation laws with stiff relaxation terms. J. Comput. Phys. 126 (2), 449–467.
Kato, M., 1995. Numerical analysis of the Nernst-Planck-poisson system. J. Theor. Biol. 177 (3), 299–304.
Larsen, E.W., Morel, J.E., 1989. Asymptotic solutions of numerical transport problems in optically thick, diffusive regimes II. J. Comput. Phys. 83 (1), 212–236.
Larsen, E.W., Morel, J.E., Miller, W.F., 1987. Asymptotic solutions of numerical transport problems in optically thick, diffusive regimes. J. Comput. Phys. 69 (2), 283–324.
MacGillivray, A.D., 1968. Nernst-Planck equations and the electroneutrality and donnan equilibrium assumptions. J. Chem. Phys. 48 (7), 2903–2907.
MacGillivray, A.D., Hare, D., 1969. Applicability of Goldman's constant field assumption to biological systems. J. Theor. Biol. 25 (1), 113–126.
Mafé, S., Manzanares, J.A., Pellicer, J., 1988. The charge separation process in non-homogeneous electrolyte solutions. J. Electroanal. Chem. Interfacial Electrochem. 241 (1), 57–77.

[4] The time step size dependency study reveals an error of approximately 1% when using this time step size.

Mafé, S., Pellicer, J., Aguilella, V.M., 1986. Ionic transport and space charge density in electrolytic solutions as described by Nernst-Planck and poisson equations. J. Phys. Chem. 90 (22), 6045–6050.
Masterov, M., 2019. Towards Industrial-Scale Bubble Columns: The Development and Application of the High Performance Computing Framework. Ph.D. thesis. Eindhoven University of Technology.
Newman, J., Thomas-Alyea, K.E., 2004. Electrochemical Systems. John Wiley & Sons. 3 edition.
Prokopenko, A., Siefert, C.M., Hu, J.J., Hoemmen, M., Klinvex, A., 2016. Ifpack2 User's Guide 1.0. Technical Report SAND2016-5338. Sandia National Labs.
Scharfetter, D.L., Gummel, H.K., 1969. Large-signal analysis of a silicon read diode oscillator. IEEE Trans. Electron Dev. 16 (1), 64–77. Conference Name: IEEE Transactions on Electron Devices.
Subramaniam, A., Chen, J., Jang, T., Geise, N.R., Kasse, R.M., Toney, M.F., Subramanian, V.R., 2019. Analysis and simulation of one-dimensional transport models for lithium symmetric cells. J. Electrochem. Soc. 166 (15), A3806.
Tang, K., Li, Z., Da Wang, Y., McClure, J., Su, H., Mostaghimi, P., Armstrong, R.T., 2023. A pore-scale model for electrokinetic in situ recovery of copper: the influence of mineral occurrence, zeta potential, and electric potential. Transp. Porous Media 150 (3), 601–626.
The Trilinos Project Team, 2020. The Trilinos Project Website. https://trilinos.github.io.